(NASA-TM-X-73232) ANALYSIS OF ABLATION DEBRIS FROM NATURAL AND ARTIFICIAL IRON METEORITES (NASA) 33 p HC A03/MF A01 N77-25033
CSCL 03B Unclas
G3/88 30342

NASA TECHNICAL MEMORANDUM

NASA TM X- 73,232

NASA TM X- 73,232

ANALYSIS OF ABLATION DEBRIS FROM NATURAL AND ARTIFICIAL IRON METEORITES

M. B. Blanchard
Ames Research Center, NASA
Moffett Field, Calif. 94035

and

A. S. Davis
San Jose State University
San Jose, Calif. 95192

May 1977

1. Report No.
NASA TM X-73,232

2. Government Accession No.

3. Recipient's Catalog No.

4. Title and Subtitle
ANALYSIS OF ABLATION DEBRIS FROM NATURAL AND ARTIFICIAL IRON METEORITES

5. Report Date

6. Performing Organization Code

7. Author(s)
M. B. Blanchard and A. S. Davis

8. Performing Organization Report No.
A-7000

10. Work Unit No.
195-21-04-02

9. Performing Organization Name and Address
Ames Research Center, NASA
Moffett Field, Calif. 94035 and
San Jose State University, San Jose, Calif. 95192

11. Contract or Grant No.

13. Type of Report and Period Covered
Technical Memorandum

12. Sponsoring Agency Name and Address
National Aeronautics and Space Administration
Washington, D. C. 20546

14. Sponsoring Agency Code

15. Supplementary Notes

16. Abstract

Artificial ablation studies have been performed on iron and nickel-iron samples by using an arc-heated plasma of ionized air. Experiment conditions simulated a meteoroid traveling about 12 km/sec at an altitude of 70 km. The artificially produced fusion crusts and ablation debris show features very similar to natural fusion crusts of the iron meteorites Boguslavka, Norfork, and N'Kandhla and to magnetic spherules recovered from Mn nodules. X-ray diffraction, electron microprobe, optical, and scanning electron microscope analyses revealed that important mineralogical, elemental, and textural changes occur during ablation. Some metal is melted and ablated. The outer margin of the melted rind is oxidized and recrystallizes as a discontinuous crust of magnetite and wustite. Adjacent to the oxidized metallic ablation zone is an unoxidized metallic ablation zone in which structures such as Widmannstatten bands are obliterated as the metal is transformed to unequilibrated α_2 nickel-iron. Volatile elements such as S and P are vaporized. Less volatile elements such as Si and Mn undergo fractionation and are concentrated in the oxide phases while Ni is concentrated in the metal phases. Dissimilar phases form an intimate intergrowth that persists to a submicroscopic level. Identification of meteor ablation debris in particle collections cannot be based on a single parameter, but elemental, mineralogical composition as well as morphological and textural features must be considered.

17. Key Words (Suggested by Author(s))
Cosmic dust
Interplanetary dust
Meteorite ablation
Spherules
Atmospheric particles

18. Distribution Statement
Unlimited

STAR Category — 88

19. Security Classif. (of this report)	20. Security Classif. (of this page)	21. No. of Pages	22. Price*
Unclassified	Unclassified	31	$3.75

*For sale by the National Technical Information Service, Springfield, Virginia 22161

INTRODUCTION

Results of the Smithsonian Institution's program on short-lived phenomena (1970) indicate that large quantities of cosmic matter reach the earth. The Prairie Network in the U.S. (1964 to 1975) and the All-Sky Network in Czechoslovakia (1958 to date) observed hundreds of bright meteors, but very few meteorites were recovered [McCrosky et al., 1971]. Apparently, most meteoroids are totally ablated in the atmosphere and, hence, large quantities of ablation material must reach the earth's surface in a finely divided state. Many attempts have been made to collect meteor ablation debris and submicron cosmic dust. Collections have been made from Greenland ice [Langway and Marvin, 1964], deep sea sediments [Schmidt and Keil, 1966], deep sea manganese nodules [Finkelman, 1972], and Paleozoic salt deposits [Mutch, 1966]. Atmospheric collections have been made with sounding rockets [Farlow et al., 1970], balloons [Brownlee and Hodge, 1969, 1973], and high altitude aircraft [Carr, 1970]. Regardless of source or method of collection in each study, the main difficulty was distinguishing between terrestrial contaminants and actual cosmic matter.

In order to gain a better understanding of the ablation process and to develop new criteria for identification of ablation debris, Blanchard [1969, 1974] began a systematic ablation study. Carefully analyzed mineral samples were subjected to ablation conditions that simulated meteor entry into the upper atmosphere. Studies with iron oxides [Blanchard, 1972] and olivine [Blanchard and Cunningham, 1974] indicated that several different chemical processes were involved. Wustite was formed, indicating reducing conditions in some instances. Volatile elements such as S, P, and Cl were depleted. Hydrated minerals, such as serpentine, were destroyed in the ablation zone. A significant amount of iron in the olivine was oxidized to form magnetite, producing a more Mg-rich olivine in the fusion crust. In both the iron oxides and the olivine samples a distinctive texture developed, consisting of a myrmekite-like intergrowth of magnetite lamellae with glass or olivine, that was indicative of the ablation environment. These results were found to be consistent with fusion crust studies of Allende, Murchison, and Orgueil meteorites [Blanchard and Cunningham, 1974; Blanchard et al., 1974; Brownlee et al., 1975].

The purpose of this study is to characterize the chemical, mineralogical and textural changes in iron and nickel-iron samples that were subjected to artificial meteor ablation, and to relate these results to fusion crusts of three natural iron meteorites (Boguslavka, Norfork, and N'Kandhla) and to meteoritic spherules recovered from deep sea Mn nodules.

EXPERIMENTAL METHODS

The ablation simulation was performed in a constricted-arc supersonic jet facility described by Shepard et al. [1967]. Facility conditions can be varied to simulate a wide range of velocities and altitudes; but for these experiments, the conditions established simulated a low-velocity meteor traveling with a velocity of 12 km/sec at an altitude of 70 km. Meteor passage was simulated by placing the samples into a plasma beam of ionized air, argon, and electrons. Metallurgical iron (~99% Fe) and nickel-iron (~10% Ni) alloys containing traces of Mn, Cr, V, and Si were used for this ablation experiment. Ablation lasted for about 30 sec. The ablated material was collected on a water-cooled collector. The remaining samples, with flanges of ablated material adhering to the sides, were also recovered for analysis. Extensive analyses were conducted on the iron and nickel-iron samples, fusion crusts, and ablated particles to characterize the morphological, elemental, and mineralogical changes. The natural fusion crusts of the three iron meteorites and eight magnetic spherules from Mn-nodules were analyzed for comparison. Textural and morphological features were examined by optical and scanning electron microscopy (SEM). Since the SEM (Joelco-JSMU-3) is equipped with an energy dispersive x-ray detector, qualitative elemental analyses could be performed on small-scale intergrowths. Quantitative elemental analysis of the bulk composition of the unablated iron and nickel-iron samples were made by wet chemical analysis and emission spectroscopy. All other determinations of elemental content of all phases present were made with the electron microprobe (M.A.C.-400), by using a LiF analyzing crystal and a sealed proportional detector for Fe, Ni, Cr, Mn, and V, and by using an ADP analyzing crystal and gas-flow proportional detector for elements with lower atomic number. Analyses for Fe, Ni, Cr, Mn, and V were conducted with an accelerating potential of 25 kV, while 15 kV were used for Si. Pure elemental standards, as well as chemically analyzed bulk samples, were used as standards. Corrections for drift, background, and detector dead time were applied to all data. Absorption corrections were made by using the method outlined by Adler and Goldstein [1965], but using Heinrichs [1966] mass absorption values. X-ray fluorescence corrections were made according to Colby's [1966] procedure. Atomic number corrections were made according to procedure described by Thomas [1964].

Minerals present in the unablated and artificially ablated samples, in the natural meteorites and their fusion crusts, and in the spherules from Mn-nodules were identified by x-ray diffraction using Debye-Scherrer powder diffraction techniques described by Blanchard [1972].

EXPERIMENTAL RESULTS

Artificial Ablation

Fusion crust. The original iron and nickel-iron samples were nearly pure metallurgical iron alloys that contained only traces of Si, Mn, Cr, and V. Optically, both samples exhibited smooth homogeneous surfaces, and x-ray diffraction revealed only one crystalline phase corresponding to α-iron. In the nickel-iron sample (~10% Ni), this must be the distorted, body-centered α_2 form since the normal, body-centered form can accommodate only up to 7.5% Ni. In a nickel-iron melt that contains anywhere from 7% to 30% Ni, γ Ni-Fe will be the only phase present above a temperature of about 800° C. If the alloy is rapidly quenched, the face-centered γ phase transforms to the unequilibrated α_2 form. Isothermal cooling or mild reheating decomposes the α_2 into a fine-grained mixture of α and γ, known as plessite. The alternating bands of α and γ nickel-iron that constitute the well-known Widmannstatten structures in octahedrites are the result of a slow diffusion process acting over long periods of time. The γ phase, when present, is easily identified by x-ray diffraction, but the α_2 form is distinguishable from the normal α form only by line broadening in the diffraction pattern.

During ablation, droplets of melted alloy fell off, while others formed flanges adhering to the flanks of the samples. A thin (50-80 μm), discontinuous fusion crust, composed mostly of an intergrowth of magnetite with an amorphous, glassy phase, formed along the outer surface of the bulk samples. Several magnetite grains were observed that have a Cr-rich core. Adjacent to the fusion crust is a heat-affected transition zone (~200 μm) in which oxide patches, mostly circular in shape, are exsolved from the metallic phase (Figure 1).

Table 1 shows the elemental composition of the metal samples before and after ablation. The metal that was melted during ablation and recrystallized as a vesicular mass of droplets at the flanks of the samples was depleted in Si and Mn with respect to the unablated metal. Table 2 shows the elemental composition of the three new phases formed in the fusion crust of the iron sample. The three newly formed phases are magnetite, a Cr-rich phase that constitutes the core of several magnetite grains, and a glassy, dark-gray phase of highly variable composition (Figure 2). Heterogeneous textures persisting to a submicroscopic level are probably responsible for variations in elemental abundance measured with the microprobe. Similar phases that contained traces of Ni were observed with the SEM in the fusion crust of the nickel-iron samples, but these, generally, were not large enough for microprobe analysis.

Ablated particles. The most distinctive feature of the ablation debris is the obvious appearance of melted products. More than 90% of all ablation particles are aggregates of spherules or single spherules, in contrast to the olivine ablation experiment where spherical particles represented only 26% of those recovered [Blanchard and Cunningham, 1974]. Ablation particles are typically of two types: (1) the most abundant type is a metallic core surrounded by an iron oxide shell (Figure 3a); (2) the other type is a glassy material that contains many small metal or iron oxide inclusions (Figure 3b).

The minerals identified by x-ray diffraction in over 400 ablation particles are listed in Table 3. The most common mineral association found in an individual spherule is that of an α-iron metal core surrounded by a shell consisting of magnetite and Wustite. Traces of hematite, goethite, akaganeite, and lepidocrocite were found with some of these particles but these traces are believed to be post-ablation alteration products. Hematite has been found as a primary mineral in ablation debris, depending upon the level of oxygen available at the time of melting. In these simulated ablation experiments, the partial pressure of oxygen was too low for primary Fe_2O_3 to form. The hematite occurred only in rust-brown particles and always in association with goethite and/or akaganeite.

The glassy spherules, which constitute approximately 10% or less of all of the ablation debris, were typically amorphous and yielded weak α-iron or magnetite patterns only when they contained abundant metallic inclusions. Two glassy spherules were found that gave a weak but distinctive fayalite pattern.

Fusion Crusts of Natural Iron Meteorites

The fusion crusts of three iron meteorites — Boguslavka (H, Gp. IIA, ~5.5% Ni) [Wasson, 1974] (see Figure 4), Norfork (Om, Gp. IIIA, 7.8% Ni) [Wasson, 1974] (see Figure 5), and N'Kandhla (Om, Gp. IID, 9.9% Ni) [Wasson, 1974] (see Figure 6) — were analyzed for comparison with those artificially produced. The natural fusion crusts are discontinuous, vesicular, iron-oxide shells with occasional metal inclusions; the shells range in width from about 50 μm to over 300 μm. Adjacent to the oxide ablation zone is a heat-affected, metallic transition zone, ranging from several hundreds of microns to several millimeters, in which structures such as Widmannstatten bands, troilite inclusions, and schreibersite lamellae are wholly or partly destroyed (Figure 7). Widmannstatten bands are composed of alternating bands of α Ni-Fe (kamacite) and γ Ni-Fe (taenite) which both, upon heating and rapid cooling, transform to the unequilibrated α_2 Ni-Fe form. Troilite (FeS) and schreibersite $(Fe_2Ni)_3P$ are either completely melted, leaving large cavities, or if only partly melted, recrystallized to a fine-grained aggregate.

The minerals identified by x-ray diffraction of shavings from the fusion crusts are listed in Table 3. The predominant phases are α-iron, magnetite, and wustite. The α-iron diffraction pattern shows some line broadening when compared with the α-phase from the corresponding meteorites' interior, but the presence of the γ phase indicates that at least portions of the α_2 have decomposed to α and γ. Hematite was present in small amounts in all three of the fusion crusts but, in Boguslavka and N'Kandhla, it appeared as rust-brown, secondary alteration products, whereas a segment of Norfork fusion crust contained primary hematite (see Figure 5).

Magnetic Spherules From Mn Nodules. Eight spherules recovered from deep sea Mn nodules were analyzed for comparison with natural and artificial meteor ablation products. The black, magnetic spherules were composed of either magnetite only or a mixture of magnetite and wustite. One spherule yielded, in addition, a weak hematite diffraction pattern, but the hematite is clearly a secondary alteration product (see Table 3). Sectioned spherules showed numerous cavities and, in some instances, off-centered metallic cores rich in nickel (up to 70%) (Figure 8).

DISCUSSION

The natural fusion crusts are wider and appear optically much more homogeneous than the simulated ones. Typically, they are almost entirely composed of magnetite, with only occasional metal inclusions, but show much greater abundance of vesicles. These differences can be easily explained by different degrees of oxidation. In the simulated ablation experiment, the oxygen pressure was static, simulating conditions at 70-km altitude, whereas natural ablation conditions are much more dynamic, with oxygen pressure increasing continuously as the meteoroid penetrates deeper into the atmosphere. Oxidation of individual spherules, produced by simulated ablation, appears to have been more effective than that of the flanges and fusion crust remaining on the original samples. In fact, the ablation spherules composed of a metallic core and oxide shell are, on a smaller scale, almost a perfect duplication of natural fusion crusts (compare Figure 3a with Figures 4a, 6a, and 6b). During an actual ablation, oxygen pressures must vary considerably in different regions of the meteorite (because of the irregular shapes of some meteorites) and thereby create local turbulent flow. One segment of the Norfork fusion crust contains primary hematite (Figures 5a, 5b), which is probably the result of a local occurrence of a greater partial pressure of oxygen. According to Ramdohr [1967] and Buchwald [1975], natural fusion crusts of iron meteorites are composed predominantly of magnetite with minor amounts of wustite and only rarely hematite.

X-ray diffraction indicated the presence of wustite in many particles that optically appeared to be only a homogeneous magnetite. The spherule shown in Figure 3a optically appears to have a homogeneous magnetite shell, but x-ray diffraction produced a good wustite diffraction pattern. The wustite was resolved with the SEM (Figures 9a, 9b). Every occurrence of wustite observed in this study appeared as an intimate intergrowth with magnetite around the periphery of spherules, and was typically very difficult to identify with the optical microscope. Although a distinctively different occurrence of wustite in the form of easily visible skeletal intergrowth in the center of a magnetite spherule has been previously described [El Goresy, 1967], none of the wustite found in this study occurred in this fashion.

CONCLUSIONS

The fusion crusts of natural meteorites have mineral compositions very similar to those of artificially ablated meteorites and also to spherules recovered from Mn nodules. The entire ablation process can be summarized in several steps, with implications that should be considered when analyzing extraterrestrial particulate matter (especially particles collected from the stratosphere):

1. Melting at high temperatures and rapid cooling results in melt features and preservation of disequilibrium mineral phases such as α_2-iron and wustite.

2. Distinctive textures are produced by intergrowth of dissimilar phases that may be submicroscopic and require scanning electron microscopy for identification.

3. Volatile elements such as S, P, C, Cl, etc., are vaporized. Some of these may recrystallize along fractures in the fusion crust; some must recrystallize in the atmosphere and may be included in some of the high altitude, atmospheric collections.

4. Less volatile elements undergo fractionation and concentration in some phases according to their affinity for oxygen. In other words, the spherules formed in the early stage of ablation may be less oxidized and compositionally different than the fusion crust of the later-ablated material. The most immediate implication of this is that only indirect extrapolation concerning composition of the parent meteorite can be made from the ablation debris. With respect to particle collections, it would imply that extraterrestrial origin need not be ruled out for iron spherules with small amounts of Mn and Si as those described by Marvin and Einandi [1967] and by Millard and

Finkelman [1970]. These particles may represent early fractionation from an iron meteorite, since Si and Mn are concentrated in the early formed ablation products. Elements like Ni and Co tend to become concentrated in the metallic phases due to preferential oxidation of iron. However, the great Ni concentration observed in one of the spherules from Mn nodules, and similar ones reported by Florenskiy and Ivanov [1970] and El Goresy [1968], may be the ablation product of an Octahedrite (i.e., a melted taenite band) or even a nickel-rich ataxite. No nickel-enriched cores were observed in the artificially ablated nickel-iron sample, because oxidation was too limited. In any case, identification of extraterrestrial material cannot be based on a single parameter. Elemental and mineralogical composition, as well as morphological and textural features, must be considered.

Acknowledgments. We are grateful to W. C. A. Carlson and W. Winovich of the Ames High Enthalpy Research Branch for assistance in making the supersonic arc jet facility available for these experiments. We also thank H. Lem of LFE-Trapelo West for support with the scanning electron microscope at Ames Research Center under contract NAS2-6006. We are especially grateful to Dr. Carleton B. Moore, Center for Meteorite Studies, Arizona State University, Tempe, Arizona, for making the samples of the Boguslavka, Norfork, and N'Kandhla meteorite fusion crusts available, and to Dr. Donald E. Brownlee, Astronomy Department, University of Washington, Seattle, Washington, for the spherules from the deep sea manganese nodules. The research under this study was in part supported by NASA-Ames/San Jose State University Consortium agreement NCAR 675-414.

REFERENCES

Adler, I., and Goldstein, J. I., Absorption tables for electron probe microanalysis, NASA Tech. Note D-2984, 1965.

Blanchard, M. B., Preliminary results of artificial meteor ablation, Meteoritics, 4, 261-262, 1969.

Blanchard, M. B., Artificial meteor ablation studies: iron oxides, J. Geophys. Res., 77, 2442-2455, 1972.

Blanchard, M., Cunningham, G., and Brownlee, D.. Comparison of a fusion crust produced by artificial ablation of an olivine with fusion crusts on the Allende and Murchison meteorites, Meteoritics, 9, 316, 1974.

Blanchard, M. B., and Cunningham, G. G., Artificial meteor ablation studies: olivine, J. Geophys. Res., 79, 3973-3980, 1974.

Brownlee, D. E., Blanchard, M. B., Cunningham, G. G., Beauchamp, R. H., and Fruland, R., Criteria for identification of ablation debris from primitive meteoritic bodies, J. Geophys. Res., 80, 4917-4924, 1975.

Brownlee, D. E., and Hodge, P. W., Results of a large volume micrometeorite collection at an altitude of 115,000 feet, Meteoritics, 4, 264-265, 1969.

Brownlee, D. E., and Hodge, P. W., Ablation debris and primary micrometeoroids in the stratosphere, in Space Res., Vol. XIII, p. 1139, Adakemi Verlag, Berlin, 1973.

Buchwald, V. F., Handbook of Iron Meteorites, Their History, Distribution, Composition, and Structure, 1418 pp., Univ. of Calif. Press, Berkeley, 1975.

Carr, M. H., Atmospheric collection of debris from the Revelstoke and Allende fireballs, Geochim. Cosmochim. Acta, 34, 689-700, 1970.

Colby, J. W., The applicability of theoretically calculated intensity corrections in microprobe analysis, in The Electron Microprobe, edited by T. D. McKinley, K. F. J. Heinrich, and D. B. Wittry, pp. 95-188, Wiley & Sons, N.Y., 1966.

El Goresy, A., Electron microprobe analysis and microscopic study of polished surfaces of magnetic spherules and grains collected from the Greenland ice, Smithson. Astrophys. Obs. Spec. Report 251, 29 pp., 1967.

Farlow, N. H., Ferry, G. V., and Blanchard, M. B., Examination of surfaces exposed to a noctilucent cloud, August 1, 1968, J. Geophys. Res., 75, 6736-6750, 1970.

Finkleman, R. B., Relationship between manganese nodules and cosmic spherules, Marine Technology Jour., 6, 34-39, 1972.

Florenskiy, K. P., and Ivanov, A. V., Differentiation of meteoritic matter in the earth's atmosphere: Meteoritika, 30, 104-113, 1972. (NASA Tech. Transl. TTF-14, 138, 1972, pp. 1-17.)

Heinrich, K. F. J., X-ray absorption uncertainty, in The Electron Microprobe, edited by T. D. McKinley, K. F. J. Heinrich, and D. B. Wittry, pp. 296-377, Wiley & Sons, New York, 1966.

Langway, C. C., and Marvin, U. B., Some characteristics of black spherules, in Cosmic Dust: New York Acad. Sci., Annals, v. 119, pp. 205-223, edited by Cassidy, 1964.

Marvin, U. B., and Einaudi, M. T., Black magnetic spherules from Pleistocene and recent beach sands, Geochim. Cosmochim. Acta, 31, 1871-1884, 1967.

McCrosky, R. E., and Ceplecha, E., Photographic networks for fireballs, Smithson. Astrophys. Obs. Spec. Report 288, 18 pp., 1968.

McCrosky, R. E., Posen, A., Schwartz, G., and Shao, C. Y., Lost city meteorite — its recovery and a comparison with other fireballs, J. Geophys. Res., 76, 4090-4108, 1971.

Millard, H. T., and Finkelman, R. B., Chemical and mineralogical compositions of cosmic and terrestrial spherules from a marine sediment, J. Geophys. Res., 75, 2125-2135, 1970.

Mutch, T., Abundances of magnetic spherules in Silurian and Permian salt samples, Earth Planet. Sci. Lett., 1, 325-329, 1966.

Ramdohr, P., Die Schmelzkruste der meteoriten, Earth Planet. Sci. Lett., 2, 197-209, 1967.

Shepard, C. E., Vorreiter, J. W., Stine, H. A., and Winovich, W. I., A study of artificial meteors as ablators, NASA Tech. Note D-3740, 1967.

Thomas, P. M., A method for correcting for atomic number effects in electron-probe microanalysis, Res. Group Rept. No. AERE-R4593, United Kingdom Atomic Energy Authority, 1964.

Schmidt, R. A., and Keil, K., Electron microprobe study of spherules from Atlantic Ocean sediments, Geochim. Cosmochim. Acta, 30, 471-478, 1966.

Wasson, J. T., Meteorites — Classification and Properties, 316 pp., Springer Verlag, New York, 1974.

TABLE 1. Elemental Composition of Iron and Nickel-Iron Alloy Before and After Ablation

Element	Unablated Fe Sample	Ablated Fe Sample	Unablated Ni-Fe Sample	Ablated Ni-Fe Sample
Fe	99.1	99.8	89.9	90.8
Ni	0.08	0.08	9.7	9.9
Si	0.15	0.05	0.40	N.D.
Mn	0.10	0.01	0.15	0.02
Cr	0.10	0.08	0.07	0.07
V	0.02	0.02	0.01	0.01
S	Tr	N.D.	Tr	N.D.
P	Tr	N.D.	Tr	N.D.

Tr denotes trace and N.D. denotes not detected.

Note - all values are in weight percent.

TABLE 2. Microprobe Analysis of New Phases Formed in the Fusion Crust of the Iron Sample (wt. %)

Element	Magnetite	Cr-Rich Phase	Dark-gray, Glassy Phase
Fe	70.5 ± 2.0	30.9 ± 2.0	50.6 ± 4.0
Mn	1.0 ± 0.6	2.2 ± 0.5	5.0 ± 1.2
Cr	0.06 ± 0.05	33.8 ± 2.0	0.04 ± 0.02
V	0.04 ± 0.02	3.5 ± 1.0	0.03 ± 0.02
Si	0.15 ± 0.05	N.D.	10.9 ± 1.5

N.D. denotes not detected.

TABLE 3. Minerals Identified by X-Ray Diffraction in Ablation Products of Iron and Nickel-Iron Samples, Natural Fusion Crusts of Iron Meteorites, and Spherules From Mn Nodules

Minerals Identified	Fe Sample	Ni-Fe Sample	Boguslavka (H)	Norfork (Om)	N'Kandhla (Om)	Spherules From Mn-Nodules
Alpha Iron α Fe	H	H	H	H	H	---
Nickel-Iron γ Ni-Fe	---	L	---	L	L	---
Magnetite Fe_3O_4	M-H	M	M-H	M-H	M-H	H
Wustite* FeO	L-M	L-M	L-M	L	L	M
Hematite Fe_2O_3	L	L	Tr	L	Tr	Tr
Akaganeite β FeOOH	L	L	---	---	---	---
Lepidocrocite γ FeOOH	L	L	---	---	---	---
Goethite α FeOOH	L	L	Tr	Tr	Tr	Tr
Fayalite Fe_2SiO_4	Tr	---	---	---	---	---
Amorphous	L	L	---	---	---	---

H denotes high, M denotes moderate, L denotes low, and Tr denotes trace.

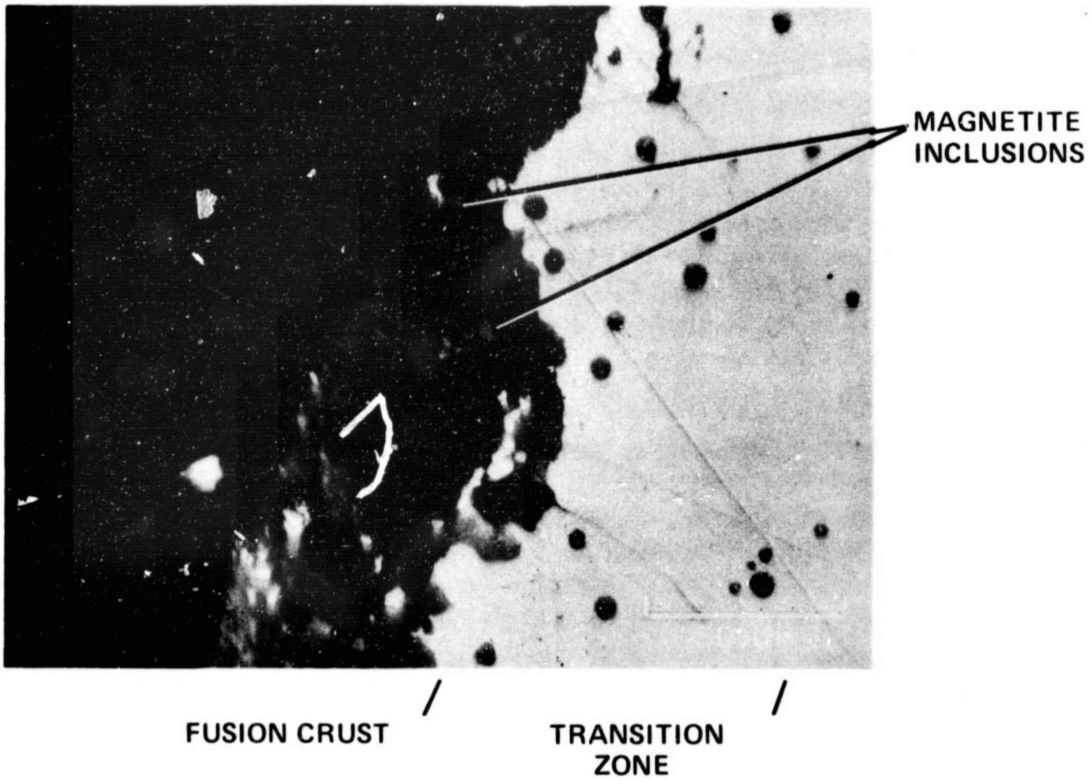

Figure 1.- Photomicrograph of the fusion crust of the iron sample. The fusion crust is mainly composed of dark-gray oxide with magnetite inclusions and a transition zone characterized by circular gray spots of oxide exsolving from the metal (white). Black areas are cavities.

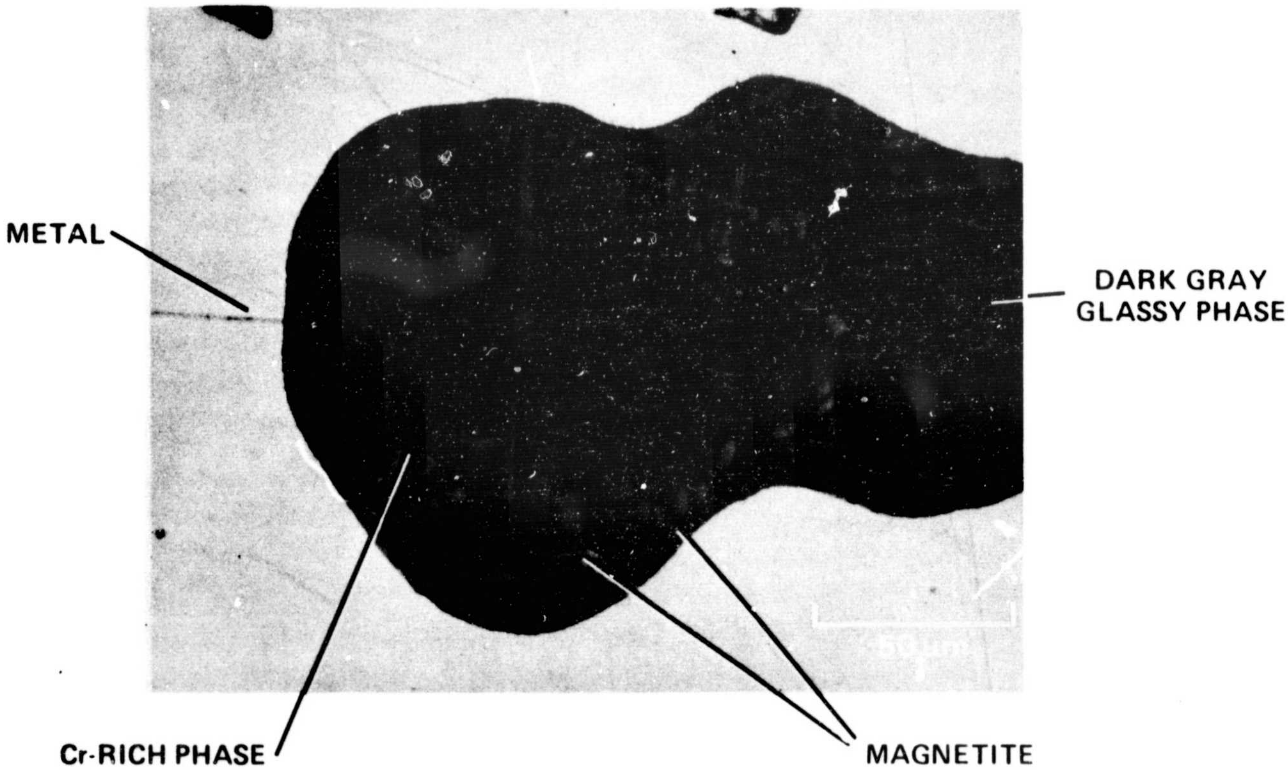

(a) Photomicrograph showing the three new phases formed during ablation: A dark-gray glassy phase, magnetite, and a Cr-rich core within a magnetite grain.

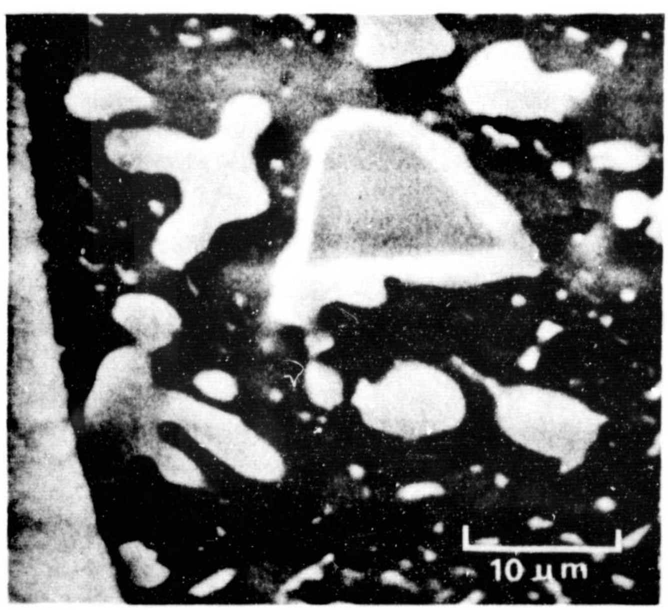

(b) Scanning electron microscope image of a magnetite grain with the Cr-rich core (shown in lower left of Figure 2a).

Figure 2.- New phases formed in fusion crust of iron sample of artificial ablation.

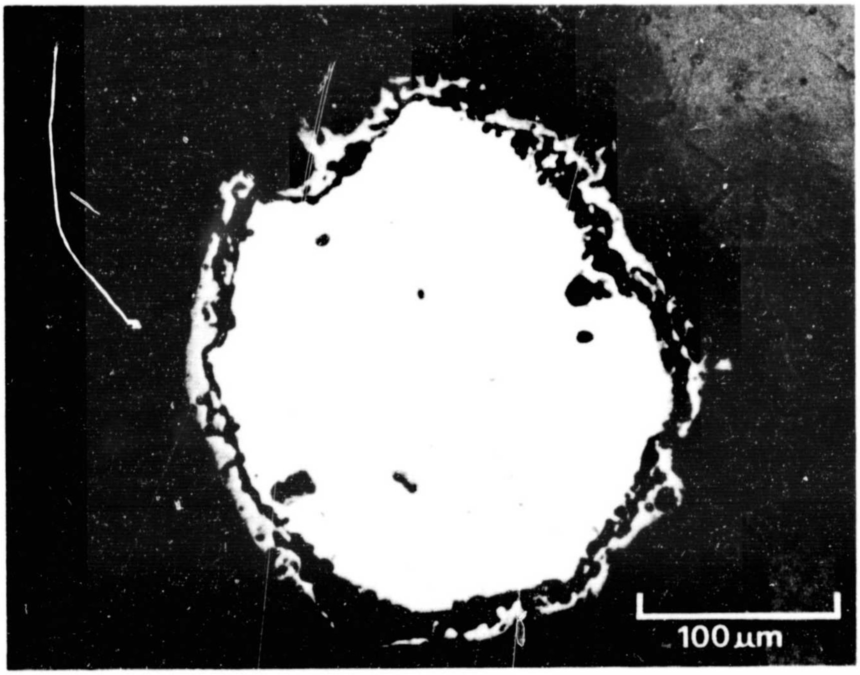

(a) Polished sections of ablation particle with a well-developed oxide shell (gray) composed of magnetite and wustite surrounding a metallic core (white).

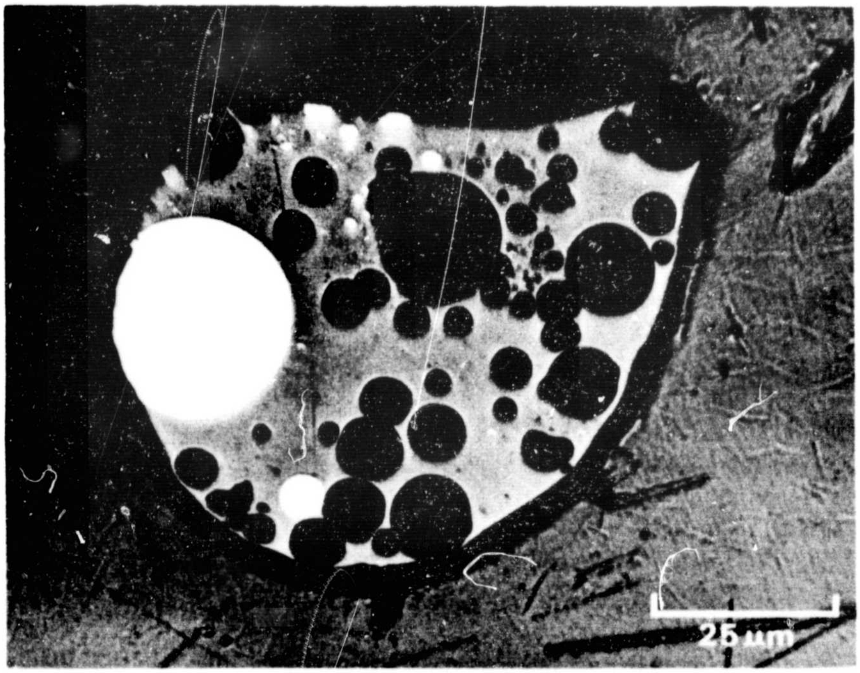

(b) Ablation particle composed of small metal spherules in a glassy matrix.

Figure 3.- Polished sections of iron and silicate ablation spherules.

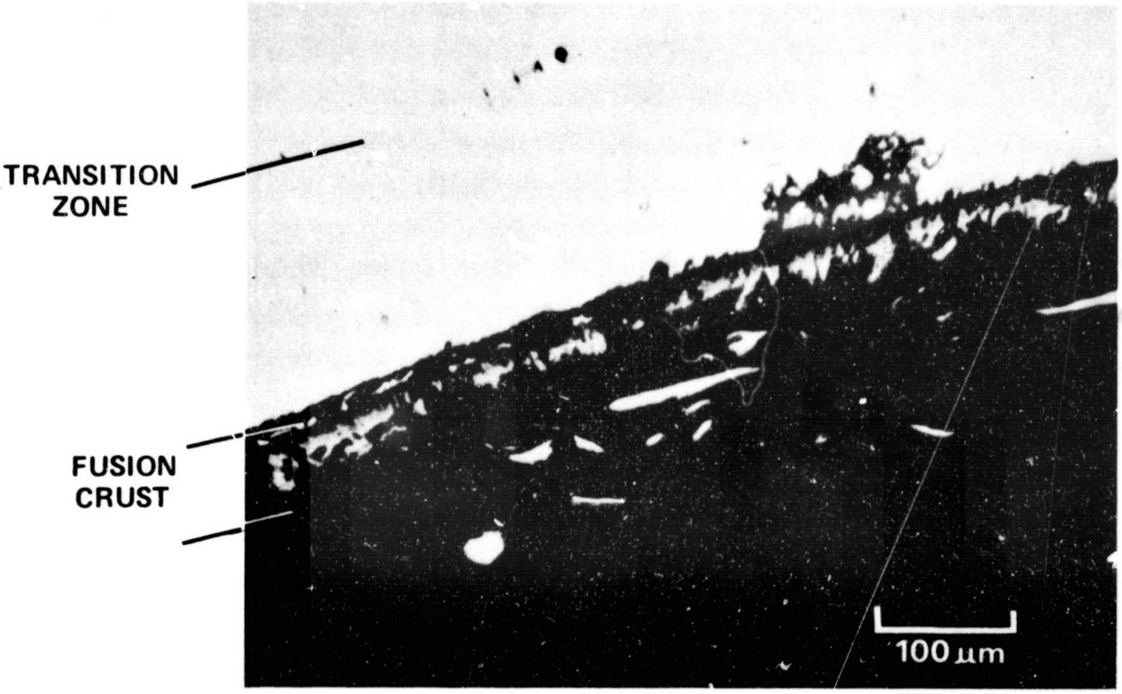

(a) Photomicrograph of the fusion crust which is composed of magnetite and wustite and a metallic transition zone adjacent to the fusion crust.

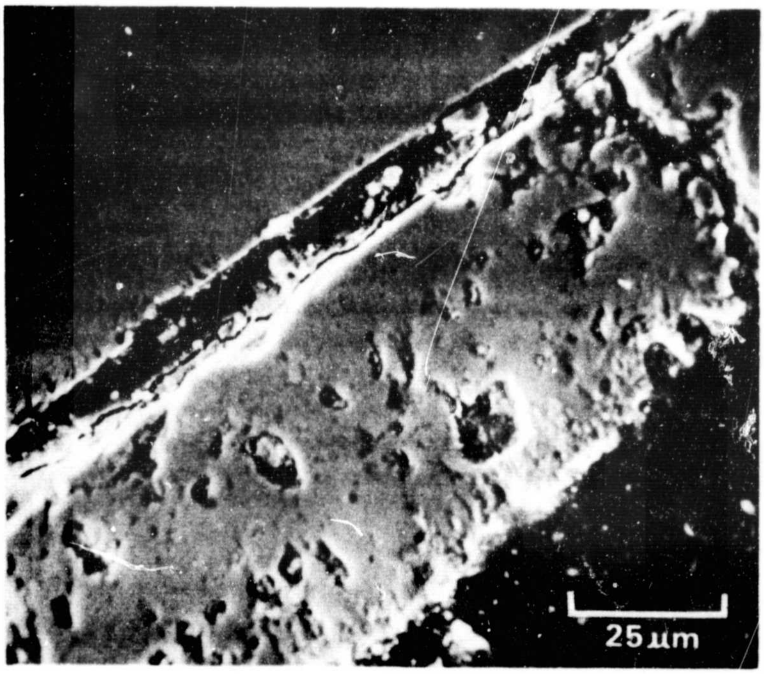

(b) Scanning electron microscope image of the fusion crust of the hexahedrite Boguslavka.

Figure 4.- Fusion crust of the Boguslavka meteorite, a hexahedrite.

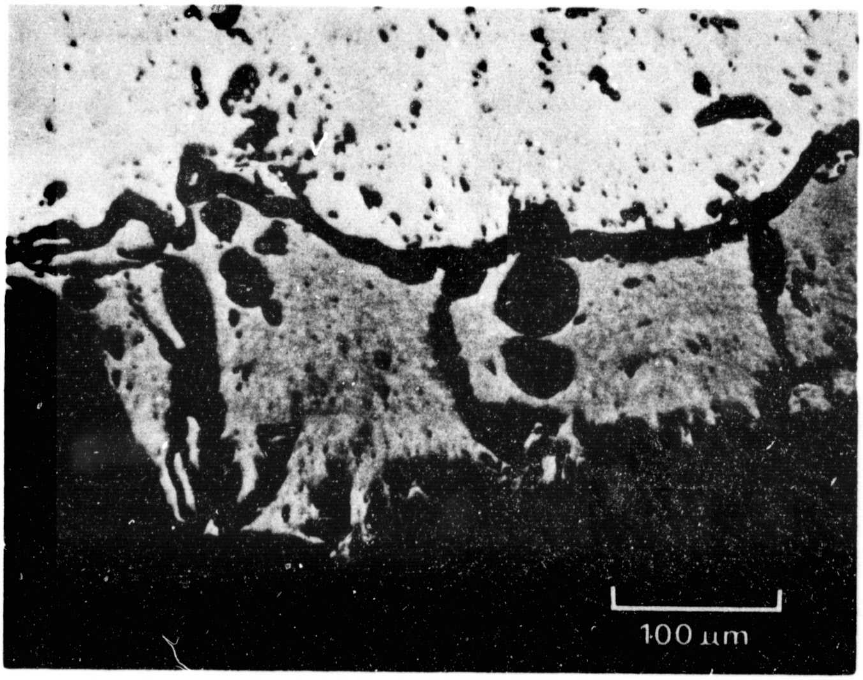

(a) Photomicrograph of the fusion crust. The fusion crust was formed on the outer flank and contains hematite inclusions (white crystals).

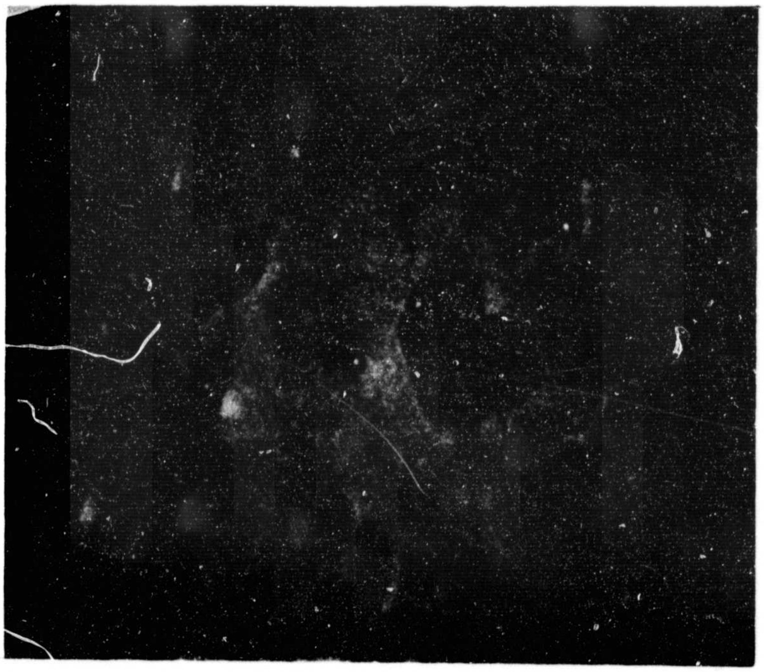

(b) SEM image of hematite inclusions in Norfork fusion crust.

Figure 5.- Fusion crust of the Norfork meteorite, an octahedrite.

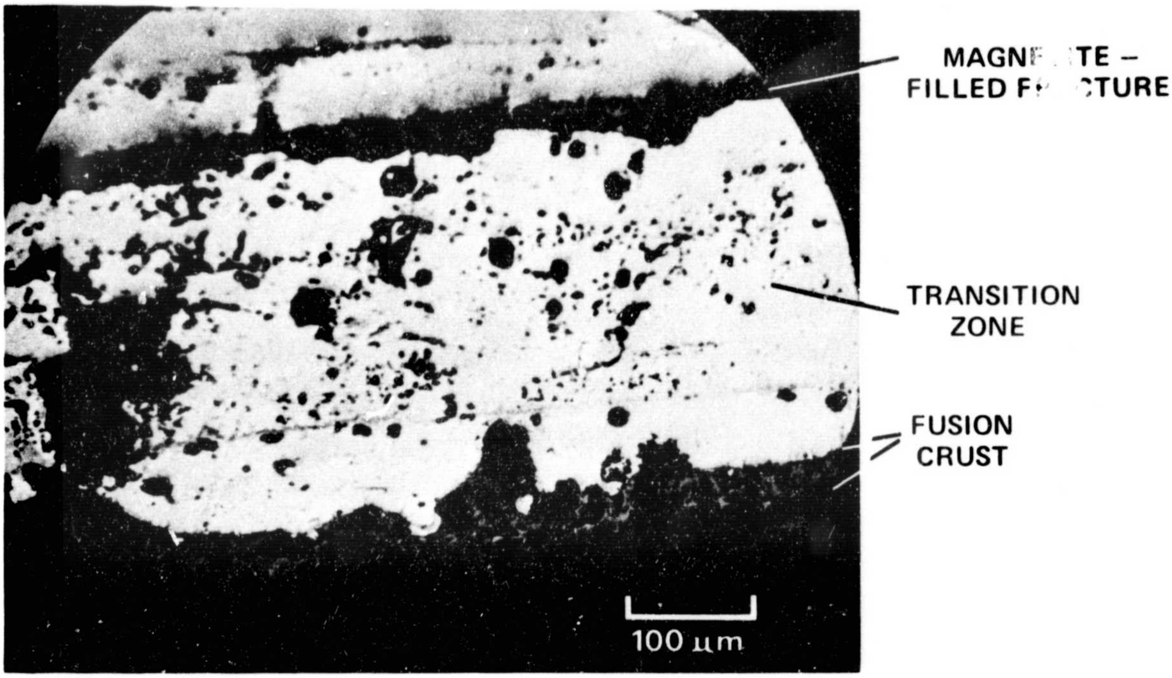

(a) Photomicrograph showing a fusion crust, transition zone in which structures have been destroyed, and a magnetite-filled fracture parallel to main crust.

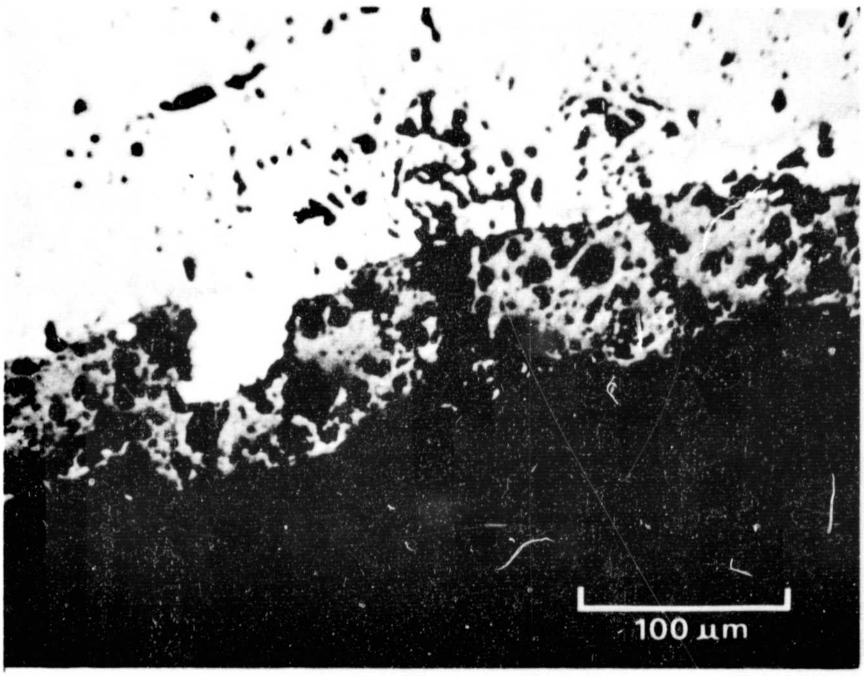

(b) Higher magnification of fusion crust.

Figure 6.- Fusion crust of the N'Kandhla meteorite, an octahedrite.

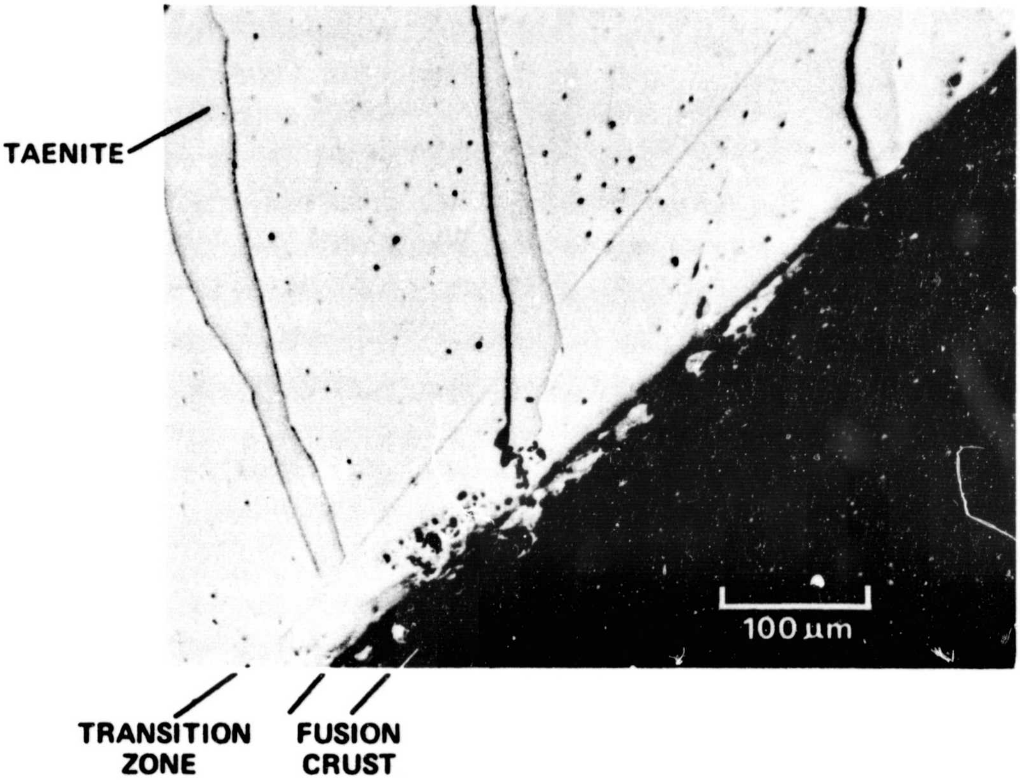

Figure 7.- Photomicrograph of the octahedrite N'Kandhla showing taenite bands, a recrystallized transition zone, and an adjacent fusion crust.

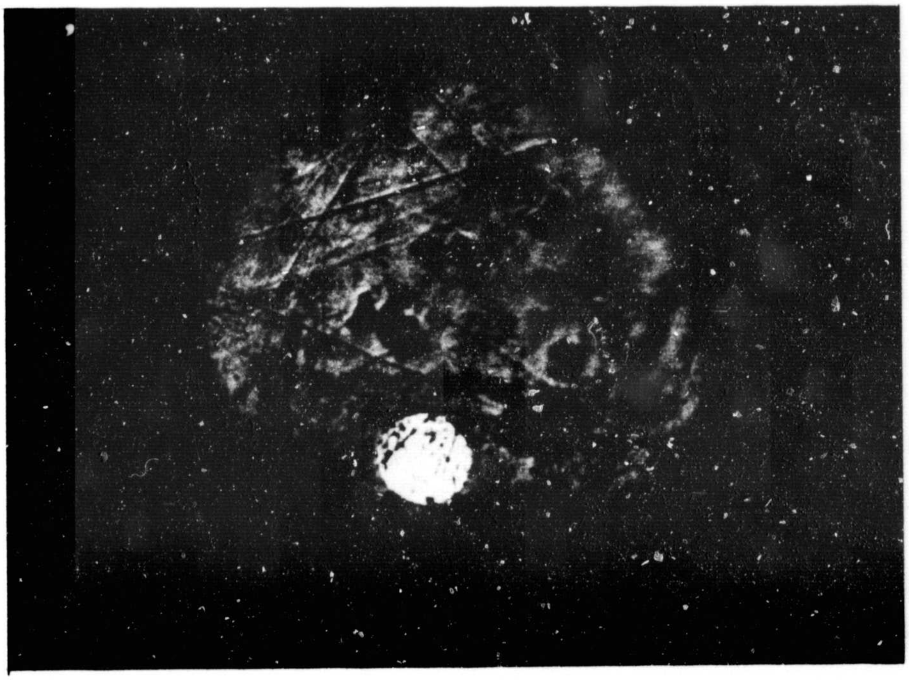

Figure 8.- Photomicrograph of polished section of a spherule (175 μm) **from a Mn nodule.** A small metal spherule (white) is embedded in a magnetite/ wustite matrix. Black areas are cavities.

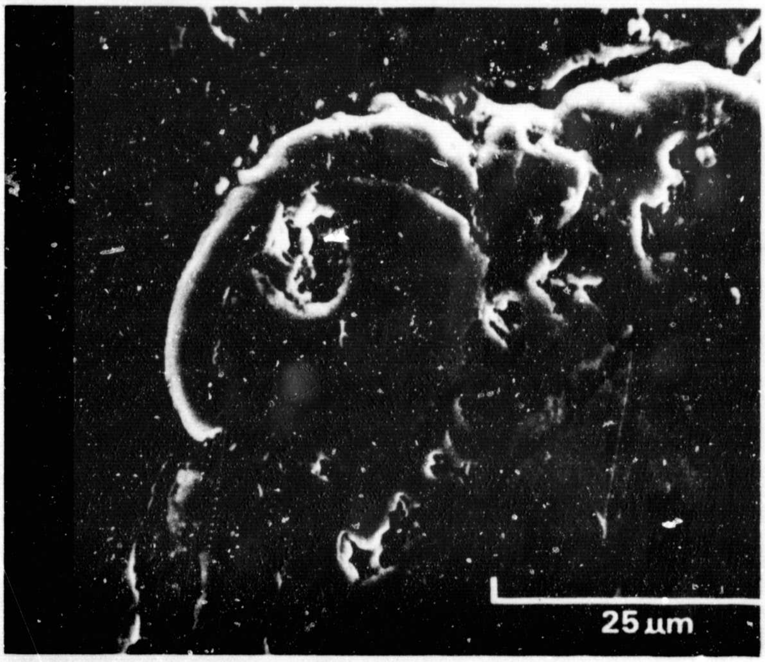

(a) Intergrowth of magnetite and wustite.

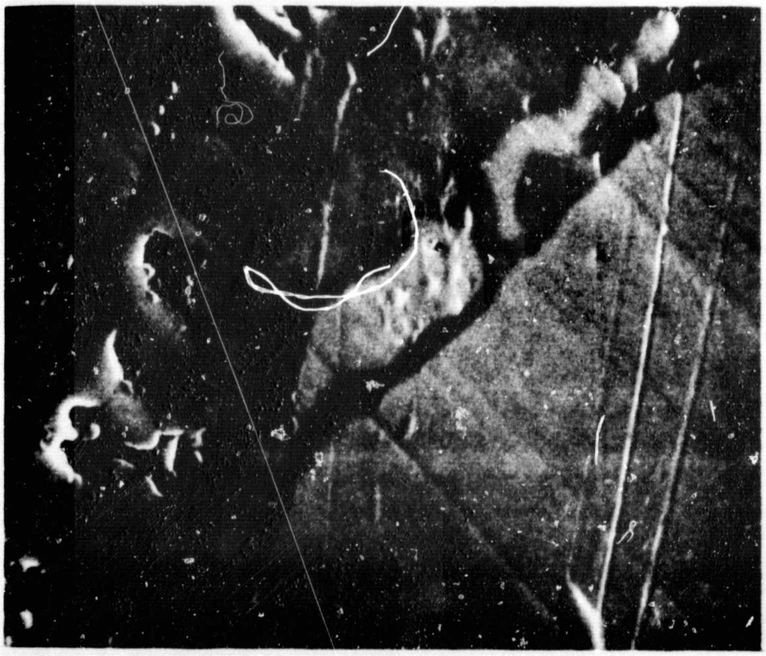

(b) Larger magnification of magnetite/wustite intergrowth.

Figure 9.- SEM image of ablation crust of the spherule shown in Figure 3a. Light area on the lower right-hand portion is unoxidized metal.

1. Report No.	2. Government Accession No.	3. Recipient's Catalog No.
NASA TM X-73,232		

4. Title and Subtitle	5. Report Date
ANALYSIS OF ABLATION DEBRIS FROM NATURAL AND ARTIFICIAL IRON METEORITES	
	6. Performing Organization Code
7. Author(s)	8. Performing Organization Report No.
M. B. Blanchard and A. S. Davis	A-7000
	10. Work Unit No.
9. Performing Organization Name and Address	195-21-04-02
Ames Research Center, NASA Moffett Field, Calif. 94035 and San Jose State University, San Jose, Calif. 95192	11. Contract or Grant No.
	13. Type of Report and Period Covered
12. Sponsoring Agency Name and Address	Technical Memorandum
National Aeronautics and Space Administration Washington, D. C. 20546	14. Sponsoring Agency Code

15. Supplementary Notes

16. Abstract

Artificial ablation studies have been performed on iron and nickel-iron samples by using an arc-heated plasma of ionized air. Experiment conditions simulated a meteoroid traveling about 12 km/sec at an altitude of 70 km. The artificially produced fusion crusts and ablation debris show features very similar to natural fusion crusts of the iron meteorites Boguslavka, Norfork, and N'Kandhla and to magnetic spherules recovered from Mn nodules. X-ray diffraction, electron microprobe, optical, and scanning electron microscope analyses revealed that important mineralogical, elemental, and textural changes occur during ablation. Some metal is melted and ablated. The outer margin of the melted rind is oxidized and recrystallizes as a discontinuous crust of magnetite and wustite. Adjacent to the oxidized metallic ablation zone is an unoxidized metallic ablation zone in which structures such as Widmannstatten bands are obliterated as the metal is transformed to unequilibrated α_2 nickel-iron. Volatile elements such as S and P are vaporized. Less volatile elements such as Si and Mn undergo fractionation and are concentrated in the oxide phases while Ni is concentrated in the metal phases. Dissimilar phases form an intimate intergrowth that persists to a submicroscopic level. Identification of meteor ablation debris in particle collections cannot be based on a single parameter, but elemental, mineralogical composition as well as morphological and textural features must be considered.

17. Key Words (Suggested by Author(s))	18. Distribution Statement
Cosmic dust Interplanetary dust Meteorite ablation Spherules Atmospheric particles	Unlimited STAR Category — 88

19. Security Classif. (of this report)	20. Security Classif. (of this page)	21. No. of Pages	22. Price*
Unclassified	Unclassified	31	$3.75

*For sale by the National Technical Information Service, Springfield, Virginia 22161